Default-Mode Activity during a Passive Sensory Task: Uncoupled from Deactivation but Impacting Activation

Michael D. Greicius and Vinod Menon

Abstract

■ Deactivation refers to increased neural activity during low-demand tasks or rest compared with high-demand tasks. Several groups have reported that a particular set of brain regions, including the posterior cingulate cortex and the medial prefrontal cortex, among others, is consistently deactivated. Taken together, these typically deactivated brain regions appear to constitute a default-mode network of brain activity that predominates in the absence of a demanding external task. Examining a passive, block-design sensory task with a standard deactivation analysis (rest epochs vs. stimulus epochs), we demonstrate that the default-mode network is undetectable in one run and only partially detectable in a second run. Using independent component analysis, however, we were able to detect the full default-mode network in both runs and to demonstrate that, in the majority of subjects, it persisted across both rest and stimulus epochs, uncoupled from the task waveform, and so mostly undetectable as deactivation. We also replicate an earlier finding that the default-mode network includes the hippocampus suggesting that episodic memory is incorporated in default-mode cognitive processing. Furthermore, we show that the more a subject's default-mode activity was correlated with the rest epochs (and ''deactivated'' during stimulus epochs), the greater that subject's activation to the visual and auditory stimuli. We conclude that activity in the default-mode network may persist through both experimental and rest epochs if the experiment is not sufficiently challenging. Time-series analysis of default-mode activity provides a measure of the degree to which a task engages a subject and whether it is sufficient to interrupt the processes—presumably cognitive, internally generated, and involving episodic memory—mediated by the default-mode network. ■

INTRODUCTION

Several studies have demonstrated that a particular set of brain regions—including the posterior cingulate cortex (PCC), the medial prefrontal cortex (MPFC), and the bilateral inferior parietal cortex (IPC), among others—consistently shows increased activity during rest or low-demand tasks compared with high-demand tasks across a wide range of cognitive experiments (Mazoyer et al., 2001; Binder et al., 1999; Shulman et al., 1997). Using quantitative positron emission tomography (PET) Raichle et al. (2001) demonstrated that these same brain regions are in metabolic equilibrium when patients rest quietly with their eyes closed. Raichle coined the term ''default mode'' to describe this network of brain regions and suggested that it was active during rest and suspended during performance of specific tasks. In a recent study, we applied a region-of-interest (ROI) functional connectivity approach to resting-state fMRI data to demonstrate that the regions constituting the default-mode network are co-active over several minutes of eyes-closed rest and during a passive, block-design, visual processing task (Greicius, Krasnow, Reiss, & Menon, 2003). We did not investigate the question of whether the network was deactivated during the visual task (i.e., suspended during flashing checkerboard epochs and active during static checkerboard epochs), but rather showed that across all epochs, BOLD signal in the PCC correlated significantly with BOLD signal in other regions in the default-mode network. In demonstrating significant inverse correlations between resting-state activity in typically activated regions in the lateral prefrontal cortex and the PCC, we suggested that deactivation may reflect a more active suppression (rather than a passive suspension) of default-mode activity.

More recently, we adapted independent component analysis (ICA) to detect the entire default-mode network en bloc (Greicius, Srivastava, Reiss, & Menon, 2004) rather than with an ROI-based approach. ICA is a statistical technique that separates a set of signals into independent—uncorrelated and non-Gaussian—spatio-temporal components (Beckmann & Smith, 2004). When applied to the T2* signal of fMRI, ICA allows not only for the removal of high- and low-frequency artifacts (Quigley et al., 2002; McKeown et al., 1998), but for the isolation of task-activated neural networks (Calhoun et al., 2002; Gu et al., 2001; McKeown et al., 1998). ICA has

Stanford University School of Medicine

also been used to detect low-frequency sensory cortex activity in fMRI data obtained during anesthesia (Kiviniemi, Kantola, Jauhiainen, Hyvarinen, & Tervonen, 2003). We have developed a template-matching procedure that allowed for the automated detection of the default-mode network during rest and during a cognitively undemanding task (button press to a visual cue) across four different groups of subjects scanned at two different institutions (Greicius et al., 2004).

Here we sought to apply ICA to an important, unanswered question pertaining to the default-mode network: whether or not activity is suppressed during the experimental periods (epochs or events) of cognitively undemanding tasks. The answer will have implications for task design and may also provide insight into the degree of cognitive load that is required to interrupt the (presumably) cognitive processes mediated by the default-mode network. McKiernan, Kaufman, Kucera-Thompson, and Binder (2003) have shown that deactivation increases across progressively more difficult tasks, but noted that even their simplest task induced significant deactivation. To explore the question of whether deactivation occurs during a cognitively undemanding task, we applied ICA to data from a passive, block-design, sensory processing task (fMRI data center accession #2-2001-111X4) (Laurienti et al., 2002). The original article compared epochs of auditory stimuli and/or visual stimuli with epochs of rest and demonstrated that the visual cortex was deactivated during auditory stimuli and conversely that the auditory cortex was deactivated during visual stimuli. In epochs where auditory and visual stimuli were presented concurrently, no sensory cortex deactivation was detected. The authors did not report the contrast comparing all seven rest epochs with all six stimulus epochs (two visual, two auditory, and two combined visual/auditory).

We hypothesized that the sensory stimuli epochs would not be sufficiently engaging to disrupt the default-mode network and that activity in the network would not fluctuate as a function of the task waveform. To prove this we show that a typical ''deactivation'' analysis of rest epochs versus stimulus epochs does not reliably yield the standard default-mode network but that the network is readily detected with ICA. The task-independence of default-mode activity is confirmed by calculating correlations between the ICA-derived time series and the task waveform. Lastly, we explore differences in activation to sensory stimuli as a function of the degree to which a subject's default-mode activity was correlated with the task waveform.

RESULTS

Task Activation/Deactivation

Contrasting stimulus epochs with rest epochs results in prominent activation of primary and secondary auditory and visual cortices (Figure 1). The reverse contrast, rest versus sensory, showed ''deactivation'' across a gigantic cluster of voxels (more than 29,000 in each run) that encompassed most of the brain and included the white matter and cerebrospinal fluid. We suspected that this largely nonneural pattern of deactivation represented ''false deactivations''(Laurienti et al., 2002; Aguirre, Zarahn, & D'Esposito, 1998) arising as an artifact of global scaling being applied to each subject's data. To confirm this, we repeated the analysis without global scaling and found that at the group level there were no significant clusters of deactivation in the rest versus sensory map for Run A. In Run B we detected five significant deactivation clusters. One was centered in the white matter and one was in the parahippocampal gyrus. The other three occurred in two typical default-mode network regions—the posterior cingulate/precuneus and the MPFC. Other typical default-mode regions—such as the inferior parietal lobes and lateral temporal lobes—were not detected. At the more stringent joint height and extent threshold of $p < .01$, there were no significant clusters of deactivation in Run A or B. Reanalysis of the group-level ''activation'' maps without global scaling was nearly identical to the analyses with global scaling, showing significant activation in the bilateral auditory and visual cortices at joint height and extent thresholds of $p < .05$ and $p < .01$.

ICA-Based Detection of the Default-Mode Network

Although there was little to no default-mode activity in the deactivation maps, using ICA we found that most subjects had a component that closely matched a standard template of the default-mode network (Figure 2A). The best-fit component shown for the subject in Figure 2A is representative. This particular component received a goodness-of-fit score of 1.28. The mean goodness-of-fit score for the best-fit components was 1.3 (standard deviation [SD] 0.31) for the 13 subjects in Run A and 1.31 (SD 0.41) for the 12 subjects in Run B. It is also important to note that although the component shown in Figure 2A was selected on a spatial basis, its temporal profile is consistent with other studies of functional connectivity in that the majority of the total power in the Fourier spectrum was in the low-frequency range (Greicius et al., 2004; Cordes et al., 2001). We derived a mean image for each subject by averaging their best-fit default-mode components from Runs A and B. In a random-effects group-level analysis, the typical default-mode network is readily identified and includes a cluster in the hippocampus (Figure 2B). Thirty-nine percent of voxels in the template used were present in the group-level map at the significance threshold used here ($p < .001$ joint height and extent). The percentage overlap increases to 78% at a less stringent threshold of $p < .05$. The 39% overlap is still considerably higher than the mean of 29% overlap across subjects observed in brain

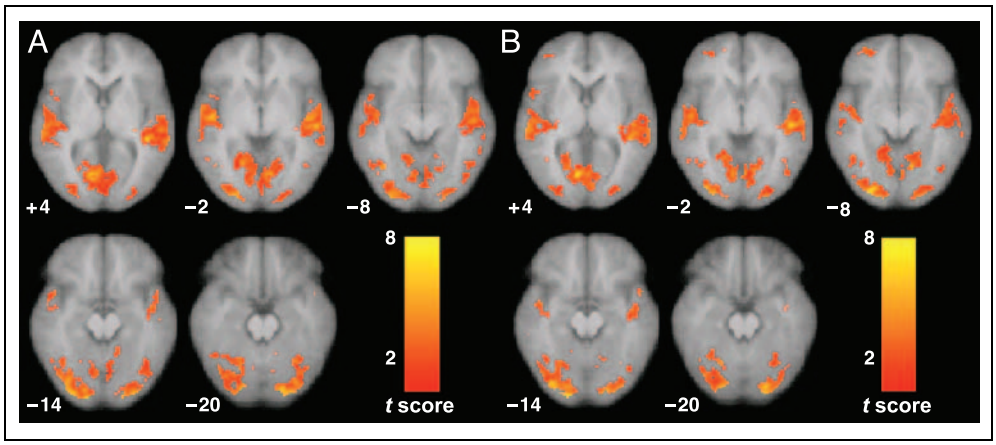

Figure 1. Activation of sensory cortices in Runs A and B. Random-effects analysis demonstrating group-level activation maps (stimulus epochs vs. rest epochs) across 13 subjects during Run A (A) and 12 subjects in Run B (B). Combined height and extent thresholds of $p < .05$ were used to determine significant clusters. The functional data are overlayed on the group-averaged structural scan in radiological convention (left side of the image corresponds to the right side of the brain). Figures below the axial images refer to the axial coordinates of MNI space.

responses to free-running audiovisual stimuli (Hasson, Nir, Levy, Fuhrmann, & Malach, 2004).

Relation between Default-Mode Activity and the Task Waveform

The presence of prominent default-mode activity across the task despite its being absent or only partially detectable in the deactivation maps suggests that, in most subjects, activity in the default-mode network was not being disrupted during the stimulus epochs. To confirm this hypothesis, we calculated correlation coefficients between the inverse task waveform (i.e., assigning rest epochs a value of +1 and stimulus epochs a value of −1) and the time series for each subject's default-mode component (separately for each of the two Runs A and B). These values provide a measure of the degree to which a subject's default-mode network activity was coupled with the task. The inverse of the task waveform was used so that positive correlations indicate increased default-mode activity during rest epochs and decreased default-mode activity during stimulus epochs. The correlation coefficients are presented in Table 1. The mean correlation across subjects between the inverse task waveform and the default-mode network time series was .09 (SD .16) for Run A and .11 (SD .2) for Run B. This low correlation between default-mode network activity and the inverse task waveform reinforces the finding that there was little (Run B) to no (Run A) deactivation in the group-level rest versus sensory contrasts. A paired *t* test comparing mean correlation coefficients in Run A (first in each subject) and Run B (second in each subject)

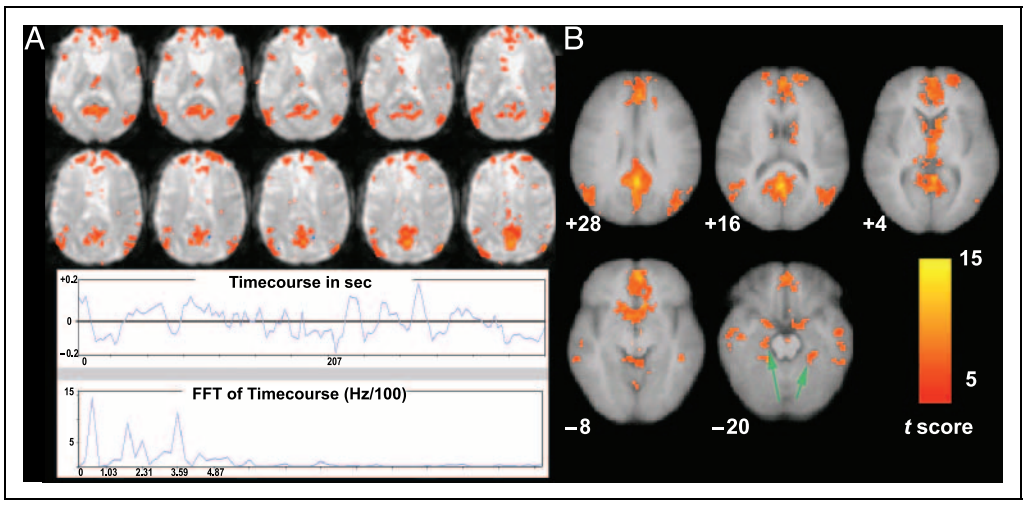

Figure 2. Default-mode activity at the individual and group levels. A single subject's default-mode component is shown in A. This component was selected, from among the subject's 26 components, as the best-fit to a standard default-mode template. The component's timecourse is shown below along with the Fourier Frequency Transformation (FFT) demonstrating the typical low-frequency oscillations seen in functional connectivity MRI analyses. The random-effects group-level analysis is shown in B. A mean image was made from each subject's two default-mode components (from Run A and Run B) and the one-sample *t* test shown in (B) was computed from the 13 mean images. The green arrows identify significant clusters in the right hippocampus and left parahippocampal gyrus (refer to Figure 1 for other details).

Table 1. Correlation Coefficients between Each Subject's Default-Mode Component Time Series and the Inverse Task Waveform

Subject Number	*Run A Correlation Coefficient*	*Run B Correlation Coefficient*
1	−.08	.03
2	−.01	0.41*
3	.07	−.01
4	−.01	.2*
5	−.04	−.02
6	.14	no data
7	.18*	.24*
8	.09	.35*
9	.23*	.27*
10	.23*	−.12
11	−.02	−.02
12	−.11	.1
13	.46*	.01

Positive correlations here signify that default-mode activity tended to be high during rest epochs and low during stimulus epochs.

*Indicates that the correlation was significant at $p < .05$.

revealed no significant differences between the two runs ($p = .68$).

Relation between Task-Related Activation and Default-Mode Activity

Lastly, we examined whether the correlation between default-mode network activity and the inverse task waveform was related to activation in visual and auditory cortices. Figure 3 shows the group activation maps for Runs A and B with each subject's correlation coefficient (from Table 1) entered as a covariate of interest. The more default-mode activity was suppressed during stimulus epochs, the greater the activation in response to auditory and visual stimuli. This is shown graphically in Figure 4 where activation extent (percentage of voxels activated) and height (mean *t* score) in the auditory and visual ROIs taken from the map in Figure 3A are plotted against the correlation coefficients for each subject. The two largest significant clusters were selected as the ROIs (see Table 2 for cluster locations).

The lack of visual cortex signal and reduced auditory cortex signal in the covariance map for Run B (Figure 3B) reflects the fact that there was attenuation of visual and auditory activation from Run A to Run B. This was confirmed in a paired *t* test where contrasting activation in Run A versus Run B revealed eight significant clusters in bilateral auditory and visual cortices, whereas there was only one significant cluster (right extrastriate cortex) in the B versus A contrast. Whereas activation attenuated over time, default-mode network activity appeared to increase from Run A to Run B. In a paired *t* test of default-mode activity, there were no significant clusters in the A greater than B contrast. In the opposite contrast, B greater than A, two significant clusters survived: a 79-voxel cluster in the MPFC (MNI coordinates of 20, 28, 50) and an 82-voxel cluster in the precuneus (0, −66, 40). Given that (1) task-related activation wanes from A to B; (2) task-related activation increases with the degree to which default-mode activity is suppressed; and (3) the measure of suppression (correlation coefficients between the inverse task waveform and the default-mode time series) is unchanged from A to B, we do not think the deactivation detected in Run B reflects increased suppression of default-mode activity during stimulus epochs. Rather, these results suggest that default-mode activity during rest epochs increases with

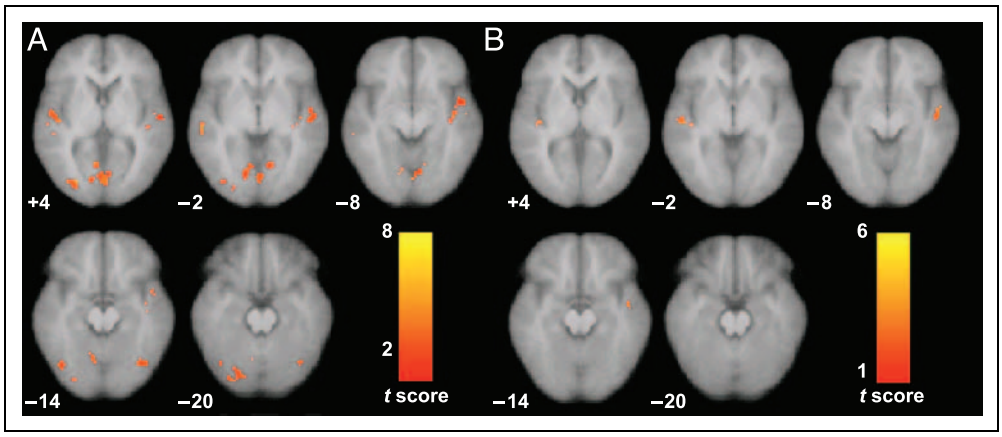

Figure 3. Suppression of default-mode activity yields increased activation to auditory and visual stimuli. A covariate-of-interest analysis showing brain regions where activation increased with increasing correlation between each subject's default-mode component time series and the inverse task waveform (see Table 1) for both Runs A (A) and B (B). The greater the degree to which default-mode activity was suppressed during the stimulus epochs, the greater the activation in visual and auditory cortices (refer to Figure 1 for other details).

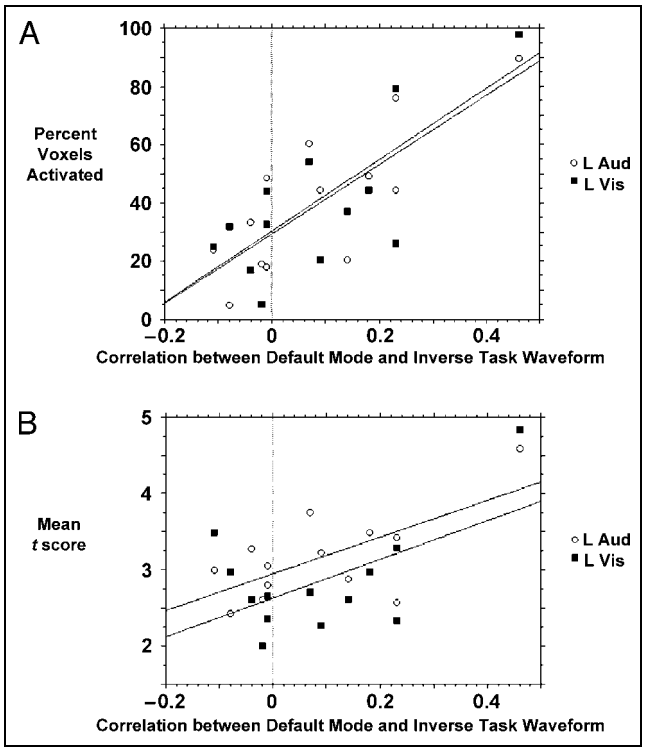

Figure 4. Activation extent and height both increase with suppression of default-mode activity. A left auditory (L Aud) and left visual (L Vis) cluster were selected from the map in Figure 3A for this confirmatory ROI analysis. Cluster size and coordinates are detailed in Table 2. The percentage of voxels activated (A) and the mean *t* score (B) within the ROI were derived for each subject and correlated with the degree to which each subject's default-mode component was suppressed during stimulus epochs (see Table 1). The correlation coefficients were .8 for left auditory and .75 for left visual in A and .66 for left auditory and .56 for left visual in B (all correlations significant at $p < .05$).

decreasing novelty of the scanning environment from Run A to Run B.

DISCUSSION

The behavioral correlates of default-mode network activity have proven difficult to identify. Raichle and colleagues have made a strong case in support of their hypothesis that the network plays an important role in monitoring and responding to both the internal milieu (Gusnard, Akbudak, Shulman, & Raichle, 2001; McGuire, Paulesu, Frackowiak, & Frith, 1996) and the external environment (Raichle et al., 2001). We have argued (Greicius et al., 2004; Greicius et al., 2003), based on the prominent role of the posterior cingulate and the, now replicated, finding of hippocampal co-activation, that the network has some relation to episodic memory. This is compatible with the hypothesis that the network mediates processes such as drawing on past experience to plan for future events (Binder et al., 1999). Retrieving information from past experiences could account for activity in two regions implicated in the default-mode network: the hippocampus (episodic memory) and the anterior temporal lobe (semantic knowledge). These hypotheses likely overlap considerably and need not be mutually exclusive. In any case, there is clearly a need for more thorough exploration of the (presumably) cognitive processes mediated by the network. This endeavor will be helped along by novel approaches, such as combined fMRI and EEG which was recently used to show that default-mode activity correlates positively with beta rhythms in the electroencephalogram (Laufs et al., 2003).

A point that is more generally agreed upon is that whatever processes the default-mode network mediates, they are interrupted when subjects are asked to attend to a demanding, externally cued task (McKiernan et al., 2003; Gusnard & Raichle, 2001; Raichle et al., 2001). We demonstrated inverse correlations during rest between the PCC and three lateral prefrontal regions activated in a separate working memory task, supporting the hypothesis that typically activated and typically deactivated brain regions exist in a dynamic equilibrium (Greicius et al., 2003). The implication is that complex cognitive processes, such as working memory, require the reallocation of neural resources from default-mode brain regions to lateral prefrontal regions. McKiernan et al. (2003) demonstrated that this reallocation of resources increases with increasing task difficulty. The current findings suggest, however, that not all tasks are sufficiently engaging to disrupt the default-mode network. The same conclusion can be drawn, in retrospect, from the study by Calhoun et al. (2002), in which default-mode activity decreased during simulated driving but not during passive viewing of the driving program.

In most subjects, there was little to no correlation between the inverse task waveform and activity in the default-mode network. This explains why, at the group level, there were no significant clusters of deactivation in Run A and only patchy deactivation in Run B that did not survive the more stringent $p < .01$ threshold. For most subjects, the sensory stimuli were attended to without disrupting default-mode activity. That is, despite the fact that default-mode activity was ongoing through the stimulus epochs, subjects still demonstrated significant activation in the visual and auditory cortices. The most striking finding reported here, however, is that the degree to which the default-mode network was suppressed during stimulus epochs correlated positively with activation in both auditory and visual cortices. We conclude that subjects were able to divide their attentional resources between simple external stimuli and the default mode, but that there was a measurable cost in reduced height and extent of sensory cortex activation to stimuli. In addition to this subject-to-subject variation, attention also varied over the course of the task such that as the task progressed subjects were less inclined to attend to stimuli and were more inclined to attend to default-mode processing. These findings have important

Table 2. Brain Regions Where Activation to Stimuli Increased with the Degree to which Default-Mode Activity was Suppressed during Stimulus Epochs in Run A

Activated Regions	*Brodmann's Area*	*Cluster Size (Voxels)*	*Maximal Z-Score Primary Peak*	*Primary Peak Location*
R Fusiform	19	57	4.59	44, −72, −18
R Sup Temporal	22	76	4.39	60, −24, 0
L Lingual*	17/18	269	4.14	−2, −82, 2
R Mid Occipital	18	80	4.01	28, −84, 4
R Sup Temporal	41	61	3.79	44, −26, 14
R Lingual	17/18	171	3.67	8, −66, 2
L Sup Temporal*	22/41	243	3.35	−46, −12, −8
R Sup Temporal	22	74	3.25	54, −10, 4
L Fusiform	19	70	3.18	−40, −68, −12
R Fusiform	19	88	3.05	22, −84, −14

These clusters correspond to the statistical map in Figure 3A.

L = left; M = middle; R = right; Sup = superior.

*Indicates the auditory and visual ROIs selected for the analysis shown in Figure 4.

implications for the interpretation of tasks with no measure of performance or attention. Individual subjects were differentially inclined to tune out their internal processing and tune in to the stimuli presentation. Furthermore, the balance shifted towards internal processing as the task progressed. These findings also suggest a means by which attention to stimuli can be gauged during passive tasks: examining correlations (or lack thereof) between a subject's default-mode time series and the task waveform.

On a more theoretical level, this work offers some new insight into the default-mode network. It would appear that many subjects were successful in dual-task processing, attending to sensory stimuli while allowing their internal cognitive processing to continue unabated. Language becomes imprecise at this stage, but one is tempted to describe this passive task as ''mindless'' except in certain subjects (13, for example) who may have ''paid more mind'' to the stimuli. In this view, the default-mode network—free-flowing until interrupted by an external task—emerges as a reasonable candidate for the neural correlate of James's (1890) stream of consciousness.

METHODS

Subjects/Stimuli/fMRI Acquisition

Thirteen healthy young subjects performed two runs (A and B) of a block-design task. Each run consisted of seven epochs of rest and six epochs of sensory stimuli (two epochs of visual stimuli, two epochs of auditory stimuli, and two epochs of mixed auditory–visual stimuli). Subjects were asked to fixate on a central crosshair and concentrate on the stimuli presented. Runs A and B had the same order of rest epochs but the order of the stimulus epochs was pseudorandomized. Functional images were acquired on a 1.5-T GE scanner using a spiral sequence (Glover & Lai, 1998) with the following parameters (TR/TE/flip angle = 3000/40/88). Structural images were acquired in the same session. Please see the original publication for further details (Laurienti et al., 2002).

fMRI Analysis

Data were pre-processed and analyzed using SPM99 (www.fil.ion.ucl.ac.uk/spm). Images were corrected for movement using least-square minimization without higher-order corrections for spin history, and normalized (Friston et al., 1995) to the Montreal Neurologic Institute template. Images were then resampled every 2 mm using sinc interpolation and smoothed with a 4-mm Gaussian kernel to decrease spatial noise.

Standard Analysis

The standard analysis was performed with SPM99. Voxelwise *t*-statistics were normalized to *z*-scores to provide a statistical measure of activation that is independent of sample size. Group whole-brain activation analysis was performed using a random-effects model using a two-stage hierarchical procedure (Holmes & Friston, 1998). In the first step, a single image was generated for each subject contrasting the six stimulus epochs with the seven rest epochs. In the second step, these contrast images were analyzed using a general linear model to determine voxelwise *t*-statistics. In order to determine the presence of significant clusters of activation, the joint expected probability distribution method (Poline,

Worsley, Evans, & Friston, 1997) was used. Group statistical maps of deactivation (rest vs. stimuli) and activation (stimuli vs. rest) were examined separately using one-sample t tests (height and extent thresholds of $p < .05$). We used one-tailed rather than two-tailed t tests because (a) we had strong a priori hypotheses about detecting activation in the sensory cortices and deactivation in the default-mode network and (b) regions of activation and deactivation are mutually exclusive. Given that the majority of the voxels in the brain (including many in white matter and ventricles) were ''deactivated'' at this threshold and that the original article reported some degree of positive correlation between global signal and the task waveform in all subjects, we suspected that these represented ''false deactivations''(Laurienti et al., 2002; Aguirre et al., 1998) resulting as an artifact of global scaling. Therefore, the group activation and deactivation maps were calculated with and without global scaling. The analyses without global scaling were performed with a joint height and extent threshold of $p < .05$ and then, in a confirmatory analysis, with a more stringent joint threshold of $p < .01$ as removing global scaling typically elevates z-scores and can result in false-positive clusters (Gavrilescu et al., 2002; Desjardins, Kiehl, & Liddle, 2001).

We also performed paired t tests (using the 12 subjects who had data for both runs) to assess differences in activation from Run A to Run B (height and extent thresholds of $p < .05$, masked to an average activation map from Runs A and B).

Independent Component Analysis

For each run in each subject, the smoothed, normalized fMRI images were concatenated across time to form a single four-dimensional image. The four-dimensional dataset was then analyzed with FSL melodic ICA software (www.fmrib.ox.ac.uk/fsl/melodic2/index.html). There is no consensus, as yet, on how to choose the optimal number of components, although methods to do so are in development (Calhoun et al., 2001). We chose to have the analysis output 26 components for each run in each subject (1/5 the number of timepoints in each run). A template of the default-mode network—derived from a group of 14 healthy young subjects in our previous study (see Figure 2 in Greicius et al., 2004)—was used to select the ''best-fit'' default-mode component from among the 26 components in each run. To do this, we developed a nonlinear template-matching procedure that involved taking the average z-score of voxels falling within the template minus the average z-score of voxels outside the template and selecting the component in which this difference (the goodness-of-fit) was the greatest. Z-scores here reflect the degree to which a given voxel's time series correlates with the time series corresponding to the specific ICA component. Although the hippocampus made up only a small percentage of the voxels in the template, to be sure we were not biasing our results towards finding hippocampal co-activation in the network, we repeated the ''best-fit'' selection process after removing the hippocampal voxels from the template. In all 25 runs, the same best-fit component selected with the original template was selected with the modified template.

To create a group-level statistical map, we first generated a mean default-mode image for each subject by averaging the default-mode component images from Runs A and B (Subject 6 only had data from Run A and this single image was used). The mean default-mode image from each subject was then combined in a second-level, random-effects analysis to generate a group statistical map for the default-mode network. Significant clusters of activation were determined using the joint expected probability distribution (height and extent thresholds of $p < .001$). We also performed paired t tests examining default-mode network activity across the two runs (height and extent thresholds of $p < .05$, masked to the average default-mode network map, Figure 2B).

Correlation Analyses

To gauge the extent to which a subject's default-mode network activity was linked to the task waveform, we calculated the correlation coefficient between the time series of the default-mode component and the inverse task waveform (task design with +1 assigned to rest epochs and −1 assigned to stimulus epochs, convolved with the canonical hemodynamic response function). This was done separately for Runs A and B in each subject. The inverse of the task waveform was used so that a positive correlation means that activity in the default-mode network increased during rest epochs and decreased during stimulus epochs. Fisher's r to z test was used to test for significance of the correlation coefficients (at the $p < .05$ level). These values were then entered into a covariate analysis in SPM99 to determine whether they correlated with activation to stimuli (i.e., whether subjects whose default-mode activity was suppressed during stimulus epochs showed greater activation to stimuli). This was done separately for Runs A and B. For the covariate analysis, significant clusters were determined using the joint expected probability distribution (height and extent thresholds of $p < .05$, minimum cluster size of 50) and masked to a group-level task activation map for the respective run (height and extent thresholds of $p < .05$, minimum cluster size of 50). Our a priori hypothesis was that the more default-mode activity was linked to the inverse task waveform, the greater the activation would be to stimuli. As such we were primarily interested in regions where activation covaried positively with the correlation coefficient. As an internal check we also ran the covariate analysis to detect regions where activation to stimuli

covaried negatively with the correlation coefficient. In this analysis, no significant clusters were detected in Run B. A single 52-voxel cluster was detected in the extrastriate cortex in Run A. This served as an ad hoc false-positive detection threshold as all significant clusters in the positive covariance analysis were greater than 52 voxels (the smallest cluster being 57 voxels and the mean cluster size being 95 voxels across 10 significant clusters).

Lastly, as a confirmatory analysis, the two largest significant clusters from the covariance analysis in Run A (one in the left auditory cortex and one in the left visual cortex) were selected as ROIs. For each subject, the correlation coefficient between the inverse task waveform and the default-mode component (reflecting the degree to which default-mode activity was suppressed during stimulus epochs, Table 1) was correlated against the percentage of voxels activated and the mean *t* score in the auditory and visual ROIs.

Acknowledgments

We thank Gaurav Srivastava for technical assistance, Paul Laurienti and colleagues for making their data available to us via the fMRI Data Center, Jack Van Horn for his help in accessing and converting the raw data, Christian Beckmann and Stephen Smith for making the FSL ICA software available, and two anonymous reviewers for their helpful comments. This study was supported by funding from the Ruth K. Broad Biomedical Research Foundation and the NIH (HD40761).

Reprint requests should be sent to Michael D. Greicius, Departments of Neurology and Psychiatry, Stanford University School of Medicine, 401 Quarry Road, MC 5719, Stanford, CA 94301-5719, or via e-mail to greicius@stanford.edu.

REFERENCES

Aguirre, G. K., Zarahn, E., & D'Esposito, M. (1998). The inferential impact of global signal covariates in functional neuroimaging analyses. *Neuroimage, 8,* 302–306.

Beckmann, C. F., & Smith, S. M. (2004). Probabilistic independent component analysis for functional magnetic resonance imaging. *IEEE Transactions on Medical Imaging, 23,* 137–152.

Binder, J. R., Frost, J. A., Hammeke, T. A., Bellgowan, P. S., Rao, S. M., & Cox, R. W. (1999). Conceptual processing during the conscious resting state. A functional MRI study. *Journal of Cognitive Neuroscience, 11,* 80–95.

Calhoun, V. D., Adali, T., McGinty, V. B., Pekar, J. J., Watson, T. D., & Pearlson, G. D. (2001). fMRI activation in a visual–perception task: Network of areas detected using the general linear model and independent components analysis. *Neuroimage, 14,* 1080–1088.

Calhoun, V. D., Pekar, J. J., McGinty, V. B., Adali, T., Watson, T. D., & Pearlson, G. D. (2002). Different activation dynamics in multiple neural systems during simulated driving. *Human Brain Mapping, 16,* 158–167.

Cordes, D., Haughton, V. M., Arfanakis, K., Carew, J. D., Turski, P. A., Moritz, C. H., Quigley, M. A., & Meyerand, M. E. (2001). Frequencies contributing to functional connectivity in the cerebral cortex in ''resting-state'' data. *AJNR American Journal of Neuroradiology, 22,* 1326–1333.

Desjardins, A. E., Kiehl, K. A., & Liddle, P. F. (2001). Removal of confounding effects of global signal in functional MRI analyses. *Neuroimage, 13,* 751–758.

Friston, K. J., Ashburner, J., Frith, C. D., Poline, J. B., Heather, J. D., & Frackowiak, R. S. D. (1995). Spatial registration and normalization of images. *Human Brain Mapping, 2,* 165–189.

Gavrilescu, M., Shaw, M. E., Stuart, G. W., Eckersley, P., Svalbe, I. D., & Egan, G. F. (2002). Simulation of the effects of global normalization procedures in functional MRI. *Neuroimage, 17,* 532–542.

Glover, G. H., & Lai, S. (1998). Self-navigated spiral fMRI: Interleaved versus single-shot. *Magnetic Resonance Medicine, 39,* 361–368.

Greicius, M. D., Krasnow, B., Reiss, A. L., & Menon, V. (2003). Functional connectivity in the resting brain: a network analysis of the default mode hypothesis. *Proceedings of the National Academy of Sciences, U.S.A., 100,* 253–258.

Greicius, M. D., Srivastava, G., Reiss, A. L., & Menon, V. (2004). Default-mode network activity distinguishes Alzheimer's disease from healthy aging: Evidence from functional MRI. *Proceedings of the National Academy of Sciences, U.S.A., 101,* 4637–4642.

Gu, H., Engelien, W., Feng, H., Silbersweig, D. A., Stern, E., & Yang, Y. (2001). Mapping transient, randomly occurring neuropsychological events using independent component analysis. *Neuroimage, 14,* 1432–1443.

Gusnard, D. A., Akbudak, E., Shulman, G. L., & Raichle, M. E. (2001). Medial prefrontal cortex and self-referential mental activity: relation to a default mode of brain function. *Proceedings of the National Academy of Sciences, U.S.A., 98,* 4259–4264.

Gusnard, D. A., & Raichle, M. E. (2001). Searching for a baseline: Functional imaging and the resting human brain. *Nature Reviews: Neuroscience, 2,* 685–694.

Hasson, U., Nir, Y., Levy, I., Fuhrmann, G., & Malach, R. (2004). Intersubject synchronization of cortical activity during natural vision. *Science, 303,* 1634–1640.

Holmes, A. P., & Friston, K. J. (1998). Generalisability, random effects & population inference. *Neuroimage, 7,* S754.

James, W. (1890). *Principles of psychology.* New York: Holt.

Kiviniemi, V., Kantola, J. H., Jauhiainen, J., Hyvarinen, A., & Tervonen, O. (2003). Independent component analysis of nondeterministic fMRI signal sources. *Neuroimage, 19,* 253–260.

Laufs, H., Krakow, K., Sterzer, P., Eger, E., Beyerle, A., Salek-Haddadi, A., & Kleinschmidt, A. (2003). Electroencephalographic signatures of attentional and cognitive default modes in spontaneous brain activity fluctuations at rest. *Proceedings of the National Academy of Sciences, U.S.A., 100,* 11053–11058.

Laurienti, P. J., Burdette, J. H., Wallace, M. T., Yen, Y. F., Field, A. S., & Stein, B. E. (2002). Deactivation of sensory-specific cortex by cross-modal stimuli. *Journal of Cognitive Neuroscience, 14,* 420–429.

Mazoyer, B., Zago, L., Mellet, E., Bricogne, S., Etard, O., Houde, O., Crivello, F., Joliot, M., Petit, L., & Tzourio-Mazoyer, N. (2001). Cortical networks for working memory and executive functions sustain the conscious resting state in man. *Brain Research Bulletin, 54,* 287–298.

McGuire, P. K., Paulesu, E., Frackowiak, R. S., & Frith, C. D. (1996). Brain activity during stimulus independent thought. *NeuroReport, 7,* 2095–2099.

McKeown, M. J., Jung, T. P., Makeig, S., Brown, G., Kindermann, S. S., Lee, T. W., & Sejnowski, T. J. (1998).

Spatially independent activity patterns in functional MRI data during the Stroop color-naming task. *Proceedings of the National Academy of Sciences, U.S.A., 95,* 803–810.

McKiernan, K. A., Kaufman, J. N., Kucera-Thompson, J., & Binder, J. R. (2003). A parametric manipulation of factors affecting task-induced deactivation in functional neuroimaging. *Journal of Cognitive Neuroscience, 15,* 394–408.

Poline, J. B., Worsley, K. J., Evans, A. C., & Friston, K. J. (1997). Combining spatial extent and peak intensity to test for activations in functional imaging. *Neuroimage, 5,* 83–96.

Quigley, M. A., Haughton, V. M., Carew, J., Cordes, D., Moritz, C. H., & Meyerand, M. E. (2002). Comparison of independent component analysis and conventional hypothesis-driven analysis for clinical functional MR image processing. *AJNR American Journal of Neuroradiology, 23,* 49–58.

Raichle, M. E., MacLeod, A. M., Snyder, A. Z., Powers, W. J., Gusnard, D. A., & Shulman, G. L. (2001). A default mode of brain function. *Proceedings of the National Academy of Sciences, U.S.A., 98,* 676–682.

Shulman, G. L., Fiez, J. A., Corbetta, M., Buckner, R. L., Miezin, F. M., Raichle, M. E., & Petersen, S. E. (1997). *Journal of Cognitive Neuroscience, 9,* 648–663.